Dynamical Behavior of Human Serum Albumin Adsorbed on or Embedded in Polyelectrolyte Multilayers

ARTICLE *in* THE JOURNAL OF PHYSICAL CHEMISTRY B · MAY 2002

Impact Factor: 3.3 · DOI: 10.1021/jp013386o

5 AUTHORS, INCLUDING:

Pascale Schwinté
French Institute of Health and Medical Resea…
30 PUBLICATIONS **1,413** CITATIONS
SEE PROFILE

Bernard Tinland
French National Centre for Scientific Research
47 PUBLICATIONS **1,390** CITATIONS
SEE PROFILE

Dynamical Behavior of Human Serum Albumin Adsorbed on or Embedded in Polyelectrolyte Multilayers

L. Szyk,[†,‡,§] P. Schwinté,[†] J. C. Voegel,[†] P. Schaaf,[*,‡] and B. Tinland[‡]

INSERM Unité 424, (UFR "Odontologie"), Université Louis Pasteur, 11 rue Humann, 67085 Strasbourg, Cedex, France, Institut Charles Sadron (CNRS-ULP), 6 rue Boussingault, 67083 Strasbourg, Cedex, France, and Home Laboratory: Institute of Catalysis and Surface Chemistry, Polish Academy of Sciences, 30-239 Cracow, ul. Niezapominajek, Poland

Received: September 5, 2001; In Final Form: January 15, 2002

We investigate the lateral diffusion of Human Serum Albumin−Fluorescein Isothiocyanate (HSA) adsorbed "on" or embedded "in" poly(sodium 4-styrenesulfonate)/poly(allylamine hydrochloride) (PSS/PAH) multilayers. Special attention is brought to the evolution of the diffusion coefficient with the surface HSA concentration. We find that while on PSS terminating films the diffusion coefficient of adsorbed HSA is independent of the protein surface concentration in the explored range, it decreases strongly with the surface concentration when HSA is adsorbed on PAH ending films. On both films, the mobile fraction of adsorbed protein molecules decreases when the surface concentration increases. At low surface coverage, up to 90% of the adsorbed protein molecules are mobile both on PSS and PAH terminating films. The decrease of the mobile fraction with the HSA surface concentration is more pronounced on PSS than on PAH reaching, respectively, 50% and 70% of mobile HSA molecules at high surface coverage. This behavior is typical for protein aggregation. Infrared spectroscopy in the ATR mode confirms the presence of protein interactions but also rules out that this constitutes the unique reason for the evolution of the mobile fraction with the surface coverage. We also find that the diffusion coefficient, at small surface concentration, is more than 1 order of magnitude smaller on PSS than on PAH ending films, the diffusion coefficients being, respectively, equal to 6.2×10^{-11} cm^2/s and 2×10^{-9} cm^2/s. A tentative model based on the wrapping of HSA molecules by PAH chains and bridging between the chains by both polyelectrolytes is proposed to explain the observed features. Finally, we also determine the diffusion coefficient of HSA embedded in PSS/PAH multilayers. We find that the diffusion coefficient of HSA embedded in −PAH−HSA−PAH-type multilayers is close to that determined when HSA is adsorbed on PAH terminating films. When HSA is embedded in −PSS−HSA-PSS-type films the diffusion coefficient is independent of the HSA surface concentration and is surprisingly slightly larger than when HSA is adsorbed on PSS terminating films, 1.1×10^{-10} cm^2/s compared to 6.2×10^{-11} cm^2/s.

Introduction

Polyelectrolyte multilayers built up by alternated depositions of polycations and polyanions constitute very powerful tools to construct targeted film coatings and in particular targeted biofilms. Different ways can be followed to achieve this goal. One can, for example, incorporate polypeptides into the films;[1] one can also adsorb or embed proteins "on" or "in" polyelectrolyte architectures resulting from strong protein interactions with polyelectrolytes.[2−4] To better control and to be able to design complex polyelectrolyte/protein biofilms, it is of prime importance to understand the rules governing the adsorption processes of proteins on polyelectrolyte multilayers. Several studies addressing different aspects of this problem were published over the past few years.

The binding between polyelectrolytes and proteins is mainly of electrostatic origin. As for protein/DNA interactions,[5] it is mainly governed by the entropy release of counterions of both the protein and the polyelectrolyte. This is illustrated by the positive binding enthalpy of poly(allylamine) with BSA at pH 7.3, indicating that the process is endothermic.[6] For the free energy of this process to become negative, the entropic contribution must be dominant. This binding is strong when the polyelectrolyte and the protein are of opposite charge. However, polyelectrolytes also interact with proteins of similar charge.[7] This is nicely demonstrated by the fact that proteins can adsorb on polyelectrolyte layers of similar charge[8,9] even if to a much smaller extent. Polyelectrolytes are also known to stabilize proteins structurally.[10,11] One observes, for example, that the incorporation of enzymes in enzyme/polyelectrolyte complexes does not alter their enzymatic activity.[4] Similar results also hold when proteins are embedded in polyelectrolyte multilayers.[12] Not only are the protein structures conserved, but also their thermal stability seems even enhanced.[13] The stabilization effect of proteins by polyelectrolytes could be due to a decrease of structural fluctuations of the protein by the surrounding polyelectrolytes. Moreover, in the case of fibrinogen embedded in the multilayers, it was also shown that the polyelectrolytes prevent the formation of intermolecular β-sheets and thus protein aggregation.[13] This can also contribute to protein stabilization.

Due to the multiple links that a protein can establish with polyelectrolytes, one could expect, at first sight, that proteins

* Author to whom correspondence should be addressed.
† Université Louis Pasteur.
‡ Institut Charles Sadron.
§ Polish Academy of Sciences.

10.1021/jp013386o CCC: $22.00
Published on Web 05/17/2002

diffuse very slowly or even remain immobile when adsorbed "on" and even more when embedded "in" polyelectrolyte multilayers. We thus undertook first measurements of the lateral diffusion coefficient of Human Serum Albumin adsorbed on or embedded in poly(sodium 4-styrenesulfonate)/poly(allylamine) (PSS/PAH) multilayers.[14] We found rather surprising results: (i) both adsorbed and embedded human serum albumin molecules can diffuse along the surface; (ii) at least two populations of adsorbed proteins exist on the top or within the multilayer architectures. One population, which represents typically 50−70% of the adsorbed proteins, corresponds to proteins that are able to diffuse laterally along the surface or in the multilayers, while the others diffuse more slowly or appear almost immobile over the experimental time scale; (iii) the diffusion coefficients of human serum albumin adsorbed on these films were of the order of $10^{-10}-10^{-11}$ cm^2/s; and (iv) the diffusion coefficient of embedded HSA was of the same order of magnitude as for the proteins adsorbed on the multilayers. These first results were obtained for high human serum albumin surface concentrations. However, it is known that the diffusion coefficient can be strongly coverage dependent, in particular due to steric hindrance effects.[15] In this paper we study the effect of the protein surface coverage on the diffusion coefficient of human serum albumin "on" and "in" polyelectrolyte multilayers. We completed the study by FTIR-ATR spectroscopy in order to investigate possible connections between the protein diffusion behavior and their secondary structure on the films. This will allow us to get additional information on the behavior of proteins adsorbed "on" and embedded "in" such films.

Materials and Methods

We used Human Serum Albumin−Fluorescein Isothiocyanate (HSA, Cat. No. A-7016 Lot No. 64H9338) and trishydroxyaminomethane (Tris) from Sigma Chemical Co., and anionic poly(sodium 4-styrenesulfonate) (MW = 70000) (PSS), cationic poly(allylamine hydrochloride) (M_n = 50000−65000) (PAH), and cationic poly(ethyleneimine) (MW = 750000) (PEI) from Aldrich. Sodium chloride was purchased from Fluka. All the chemicals of commercial origin were used without further purification. Ultrapure water from a Millipore system was used for the preparation of the buffers and solutions and for the different cleaning steps. The resistivity of the water was approximately 18 MΩ. The concentration of Tris-HCl buffer solutions was 5×10^{-4} M, and the pH was adjusted to 7.4 by addition of some droplets of concentrated HCl.

Multilayers Surface Preparation. The multilayers were built on silica microslide capillaries of rectangular shape (internal dimensions: 0.2×2.0 mm^2, length 100 mm) purchased from Wale Apparatus Co, (Hellertown, USA). The capillaries were first cleaned with a detergent solution (RBS, Roth-Sochiel Sarl, France) in an ultrasonic cleaner. Then, they were well rinsed with distilled water before being soaked in concentrated nitric acid for approximately 1 h. Each capillary was then thoroughly rinsed with ultrapure water and stored in water until use. The storage never exceeded 4 days. The multilayers were built as follows: first, the capillary was rinsed extensively with Tris-HCl buffer. The initial PEI layer was then adsorbed from a PEI solution (c_{PEI} = 5 mg/mL, 1 M NaCl). The capillary was filled with the polyelectrolyte solution with the help of a syringe and the solution was kept in contact with the capillary for 20 min. The capillary was then rinsed with 10 mL of Tris-HCl during 5 min before the PSS solution (c_{PSS} = 0.5 mg/mL, 1 M NaCl) was injected and kept in the capillary for 30 min. After rinsing with Tris-HCl, the PAH solution (c_{PAH} = 0.5 mg/mL, 1 M NaCl) was injected into the capillary and as previously, kept in contact for 30 min with the surface before being rinsed again with Tris-HCl. The same procedure was repeated by alternating PSS and PAH adsorption until the final polyelectrolyte architecture was built up. Two polyelectrolyte multilayer films were chosen: a PAH terminating film: PEI(PSS/PAH)$_3$, and a PSS terminating one: PEI(PSS/PAH)$_2$PSS.

Albumin Adsorption. HSA, at a concentration ranging from 0.005 to 0.5 mg/mL dissolved in 0.15 M NaCl 5×10^{-4} M Tris-HCl, was adsorbed on the outer layer of the polyelectrolyte film. The adsorption time chosen was always 2 h. Immediately after injection of the albumin solution into the capillary the fluorescent intensity was followed by using the FRAP equipment as a fluorometer (for details see ref 14). After 2 h of adsorption the capillary was rinsed with 10 mL of the 0.15 M NaCl Tris-HCl buffer solution at a flow rate of 0.01 mL/s, to remove from the capillary all the free and loosely bound albumin molecules. Then, the fluorescent intensity was measured again and the surface coverage of the HSA molecules Γ_{alb} was estimated from the expression:

$$\Gamma_{alb} = \frac{F_S \cdot C_b \cdot V}{F_b \cdot 2S} \tag{1}$$

where F_S and F_b represent, respectively, the fluorescent intensities [mV] on the surface and in the bulk, C_b is the bulk concentration of albumin [mg/cm^3], V is the volume of solution in the capillary [cm^3], and S is the surface area [cm^2] of the capillary illuminated by the laser beam. The factor 2 comes from the fact that the fluorescent intensity originates from both sides of the rectangular capillary. Once the adsorbed amount was estimated we determined the HSA surface diffusion coefficient.

For the measurement of the diffusion coefficient of HSA embedded in the multilayer film six further polyelectrolyte layers were deposited on the HSA ending structures. Whereas in the previous building steps of the underlying film we used polyelectrolyte solutions prepared by dissolving the polyelectrolytes in water in the presence of 1 M of NaCl, the following polyelectrolyte layers were built up from polyelectrolyte solutions in 0.15 M NaCl, 5×10^{-4} M Tris-HCl buffer. This was done in order to avoid possible albumin denaturation and led finally to PEI−(PSS/PAH)$_3$−HSA-(PAH/PSS)$_3$. PEI−(PSS/PAH)$_2$−PSS−HSA-(PSS/PAH)$_3$, PEI−(PSS/PAH)$_3$−HSA-(PSS/PAH)$_3$, and PEI−(PSS/PAH)$_2$−PSS−HSA-(PAH/PSS)$_3$ architectures.

Fluorescence Recovery after Photobleaching. The diffusion coefficients were measured by using the similar fluorescence recovery after the photobleaching technique as described in ref 14. Briefly, the diffusion coefficient of fluorescein-labeled HSA was measured by a fringe pattern fluorescence bleaching technique similar to the one described by Davoust et al.[16] The light beam of an etalon-stabilized monomode Ar laser (1 W at λ = 488 nm) was split and the two beams crossed in the capillary cell providing illumination in a deep interference fringe pattern. The fringe spacing $i = 2\pi/q$ set by the crossing angle ϕ, $q = (4\pi/\lambda)\sin(\phi/2)$, ranged from 3 to 60 μm, defining the diffusion distance. Fluorescence bleaching of the labeled species in the illuminated fringes was obtained by producing a 1-s full-intensity bleach pulse by means of Pockels's cell between nearly crossed polarizers. The experimental signal vanished because of diffusion. The decay of the amplitude of the fringe pattern of fluorescent molecules after photobleaching was detected by

modulation of the illuminating fringe position using a piezoelectrically modulated mirror and lock-in detection of the emerging fluorescence. The switching in the setup, to bleach and protect the photomultiplier, is controlled by a microcomputer that also collects the data. The use of the same fringe pattern for the bleaching and the reading ensures that they are both characterized by the same spatial wavelength which leads, for this method, to the best signal-to-noise ratio.

Davoust et al.[16] have shown that the component of the fundamental frequency of the fluorescence intensity detected in the locking-in amplifier varies with time as:

$$I_f(t) = I_1 \exp(-t/\tau) + I_0 \quad (2)$$

where I_0 (respectively, I_1) corresponds to the intensity due to the immobile (respectively mobile) proteins. The diffusion coefficient D of the labeled molecules is related to τ according to $\tau = 1/D \cdot q^2$. Measurements performed for different values of q were carried out in order to check if τ varies linearly with q^{-2} which constitutes a signature for a diffusive process. In our experiments we investigated q vectors ranging from 6000 cm^{-1} to 4500 cm^{-1} which correspond to fringe spacing i ranging from 10 μm to 14 μm. To protect the sample from photobleaching during experiments (typical duration 20 min) we used a shutter, so that the sample was only illuminated by the light during 10 s every 30 s. From the exponential decay function (2) we could also determine the mobile protein fraction f on the surface which is given by:

$$f = \frac{I_1}{I_0 + I_1} \quad (3)$$

Some Remarks about the Influence of the HSA Labeling on the Experimental Results. The labeling ratio of the HSA used was 9 fluoresceins per HSA molecule (from the manufacturer). This high fluorescein content may eventually change the interactions of the proteins with the surface. In a previous study (ref [14]) we determined the adsorbed amounts of labeled and unlabeled HSA molecules on PSS and PAH terminating films. We used the FRAP instrument as a spectrophotometer to estimate the amount of labeled HSA adsorbed and Optical Waveguide Lightmode Spectroscopy (OWLS) for the determination of the adsorbed amount of unlabeled HSA molecules. We found for identical adsorption conditions adsorbed HSA amounts of 0.23 and 0.59 $\mu g\ cm^{-1}$ (FRAP), respectively, on PSS and PAH ending films and 0.24 and 0.88 $\mu g\ cm^{-1}$ (OWLS) for unlabeled HSA molecules. The adsorbed amounts on each film are thus globally comparable for labeled and unlabeled molecules indicating that both molecule types seem to interact in a similar way with a given polyelectrolyte film. The adsorbed amount difference of 30% on a PAH terminating film can be due (i) to the fact that in OWLS one has to use a layer model to calculate the adsorbed amount and this model may not always be totally adequate; (ii) moreover, the reproducibility of adsorption experiments is usually typically of the order of 15−20% which may also affect the comparison.

A high labeling ratio may also lead to some fluorescence quenching for large surface concentrations. This could result in a decrease of the initial fluorescence contrast. This was, however, not observed in our experiments indicating that, if present, quenching remains always a small effect. Moreover, even if some quenching would be present it would not affect the mobile fraction f determined from relation (3) due to the fact that it is estimated from the ratio of the initial and final fluorescence intensity. One could also have a change in the emission efficiency of the labels when the proteins are incorporated in the films. If this would be the case one would observe a shift in the emission wavelength resulting in a color change of the film. Such a change in color was, however, never observed.

Fourier Transform Infrared Spectroscopy in ATR Mode

Fourier Transform Infrared Spectroscopy in the ATR mode was performed on an Equinox 55 FTIR spectrometer using a liquid nitrogen cooled MCT detector. Protein and polyelectrolyte solutions were prepared in deuterium oxide (99.9 atom % D, from Aldrich), using the same concentration and buffer conditions as previously described for the FRAP experiments. The solutions (about 3 mL) were flown into an overhead in-compartment ATR cell (GRASEBY-SPECAC, England), equipped with a thermally stabilized top-plate (110 μL cell volume) fitted with a 45° trapezoidal ZnSe IRE (internal reflection element) crystal (6 reflections, dimensions 72 × 10 × 6 mm^3). Samples were introduced into the cell by a peristaltic pump at a flow rate of approximately 0.25 mL min^{-1}. Single channel spectra from 512 interferograms were calculated between 400 and 4000 cm^{-1} with 2 cm^{-1} resolution using Blackman-Harris 3-term apodization and the standard BRUKER OPUS/IR software (version 3.0.4). The multilayer film was built by injecting sequentially the different polyelectrolyte solutions, each polyelectrolyte injection being followed by a rinsing step. The first polyelectrolyte layer (PEI) was adsorbed directly on the ZnSe surface. We concentrated only on the amide I band. Briefly, all processing of the infrared spectra was carried out using the SPSERV software (version 3.20, BCS Software: Dr. Csaba Bagyinka, Institute of Biophysics, Biological Research Center of the Hungarian Academy of Sciences, H-6701 Szeged, POB 521, Hungary). To eliminate water vapor contamination and to reduce noise, "Fourier smoothing" was performed on the spectra before component band analysis of the amide I band was carried out. The experiments and the data analysis were conducted similarly to what was described in details in ref 13.

One can also point out the fact that the experiments conducted in D_2O resulted in a H/D exchange of the protons of the proteins. This exchange must affect almost all the protons of the proteins as confirmed by the disappearance of the amide II band, the simultaneous appearance of the amide II′ band, and a 10 cm^{-1} shift, to lower frequencies, of the maximum of the amide I band.[17] It is, however, known that such an exchange does not affect the protein secondary structure.[17]

Results

Figures 1a and 1b represent typical evolutions of the fluorescence intensity versus time at a given incidence angle relative to experiments where HSA was adsorbed, respectively, on PSS and PAH ending films. Similar curves were obtained when HSA was embedded respectively in −PSS−HSA−(PSS or PAH)- and −PAH−HSA−(PAH or PSS)-multilayers. From these curves we deduced both $\tau(q)$ and f according to a procedure described in ref 14. We found, within experimental errors, linear variations of $1/\tau(q)$ as a function of q^2 for proteins adsorbed (Figure 2a) and embedded (Figure 2b) in polyelectrolyte multilayers. This proves that the signals originate from a Fickian diffusive process. From the slope of $1/\tau(q)$ versus q^2 we determined the diffusion coefficient of HSA. As one can see in Figure 1, one reaches a constant value for the fluorescence intensity after a long time period only when HSA is adsorbed on PAH ending films (or embedded in −PAH−HSA−(PAH or PSS)-multilayers) whereas the fluorescence intensity con-

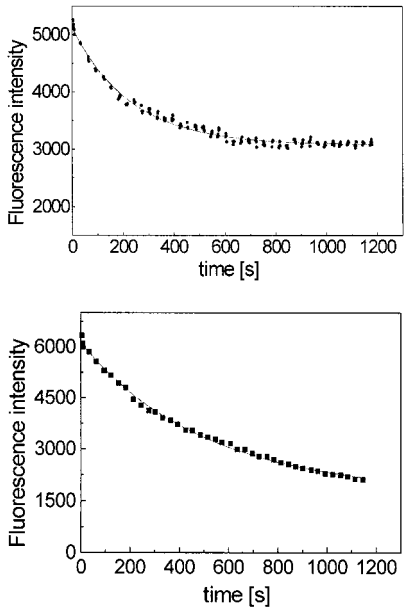

Figure 1. Evolution of the fluorescence intensity $I_f(t)$ relative to HSA adsorbed on the multilayer film as a function of time after bleaching. Points represent the experimental data, the solid lines correspond to a single-exponential fit (eq 2) of the data. (a) HSA adsorbed on a PAH terminating film; (b) HSA adsorbed on a PSS terminating film.

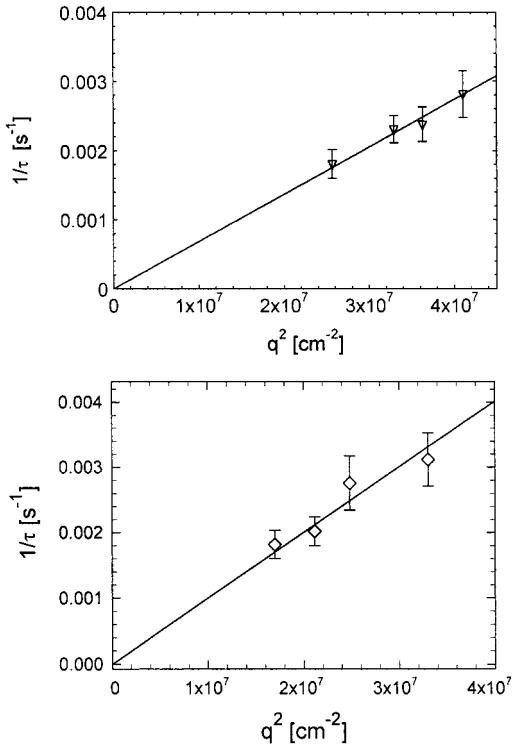

Figure 2. Typical evolution of the inverse of the decay times ($1/\tau$) as a function of q^2 for HSA (a) adsorbed on a PSS terminating film, (b) embedded in a $PEI(PSS/PAH)_2PSS-HSA-(PAH/PSS)_3$. Points represent the experimental data, the solid line represents the linear fit to the data. The slope of the line corresponds to the diffusion coefficient *D*.

tinues to decrease slightly when HSA is adsorbed on PSS ending multilayers (or embedded in −PSS−HSA−(PSS or PAH)-films). This indicates that, while on PAH we have both mobile and immobile proteins, on PSS ending films, the HSA molecules that are denoted as immobile can, in fact, slowly diffuse along the surface but at a time scale that is out of reach with our experimental setup. Thus, on PSS ending multilayers, the mobile fraction has to be considered as the "rapidly" diffusing population of HSA molecules. Table 1 gathers all the results relative to the diffusion behavior of HSA adsorbed "on" or embedded "in" PSS/PAH multilayer architectures. One can point out that all our results were obtained after 2 h of adsorption time. However, the absence of aging effects in the diffusion behavior of the HSA molecules on these multilayer films was demonstrated previously.[14]

TABLE 1: Diffusion Coefficient of HSA Adsorbed on or Embedded in PAH/PSS Multilayer Films as a Function of Surface Concentration

multilayer architecture[a]	surface concentration Γ_{HSA} (μg/cm^2)	diffusion coefficient *D* (cm^2/s) × 10^{10}	mobile fraction *f*[b]
−PAH−HSA	0.59	1.0 ± 0.1	0.7
−PAH−HSA	0.42	0.97 ± 0.08	0.7
−PAH−HSA	0.37	2.2 ± 0.3	0.7
−PAH−HSA	0.12	8.4 ± 0.5	0.8
−PAH−HSA	0.04	15.0 ± 0.1	0.9
−PAH−HSA	0.03	15.0 ± 0.2	0.9
−PSS−HSA	0.23	0.7 ± 0.1	0.4−0.6
−PSS−HSA	0.16	0.6 ± 0.1	0.5
−PSS−HSA	0.06	0.6 ± 0.1	0.6
−PSS−HSA	0.04	0.6 ± 0.1	0.9
−PAH−HSA-PAH−	0.8	1.3 ± 0.6	0.3
−PAH−HSA-PAH−	0.08	9.0 ± 0.4	0.3
−PAH−HSA-PSS−	0.82	2.7 ± 0.7	0.3
−PAH−HSA-PSS−	0.43	6.0 ± 0.2	0.4
−PSS−HSA-PSS−	0.23	1.1 ± 0.7	0.5
−PSS−HSA-PSS−	0.17	1.1 ± 0.9	0.6
−PSS−HSA-PSS−	0.12	1.0 ± 0.8	0.6
−PSS−HSA-PSS−	0.03	1.0 ± 0.5	0.7
−PSS−HSA-PAH−	0.18	1.0 ± 0.9	0.5

[a] −PAH−HSA and −PSS−HSA correspond, respectively, to the $PEI(PSS/PAH)_3-HSA$ and to the $PEI(PSS/PAH)_2PSS-HSA$ architectures; −PSS−HSA-PSS− and −PAH−HSA−PAH− correspond, respectively, to the $PEI(PSS/PAH)_2PSS-HSA-(PSS/PAH)_3$ and $PEI(PSS/PAH)_3-HSA-(PAH/PSS)_3$ architectures; −PAH−HSA−PSS− and −PSS−HSA−PAH− correspond, respectively, to the $PEI(PSS/PAH)_3-HSA-(PSS/PAH)_3$ and $PEI(PSS/PAH)_2PSS-HSA-(PAH/PSS)_3$ architectures. [b] *f* represents the fraction of rapidly diffusing molecules when HSA is adsorbed on PSS terminating films or when it is inserted in PSS−HSA−(PSS or PAH) film.

HSA Molecules Adsorbed on Polyelectrolyte Multilayers. One first observes that the mobile fraction *f* of HSA molecules adsorbed on polyelectrolyte multilayers decreases when the protein surface concentration is increased. This is valid on both PSS and PAH terminating films even if the effect is more pronounced on PSS terminating ones where the fraction of mobile proteins becomes smaller for high surface concentrations (see Figure 3). HSA molecules adsorbed on polyelectrolyte multilayers seem thus not to follow the observed independence of *f* with the protein surface concentration found for the mobile fraction of BSA molecules adsorbed on solid or polymeric surfaces.[15,18] Moreover, for low protein surface coverage, the mobile fraction becomes of the order of 90% whereas on solid surfaces one usually reports values of the order of 40%.[18] On solid surfaces the independence of *f* with the coverage is explained by an heterogeneity of protein conformations or orientations in the adsorbed state. In the present case the existence of at least two populations could originate from possible interactions between HSA molecules on the surface leading to large aggregates. An increase of the fraction of aggregated molecules is indeed expected when the surface coverage increases.

One of the most striking features that emerges out of Table 1 is that the diffusion behavior of HSA is entirely different when it is adsorbed on PSS or on PAH ending multilayers. On PAH

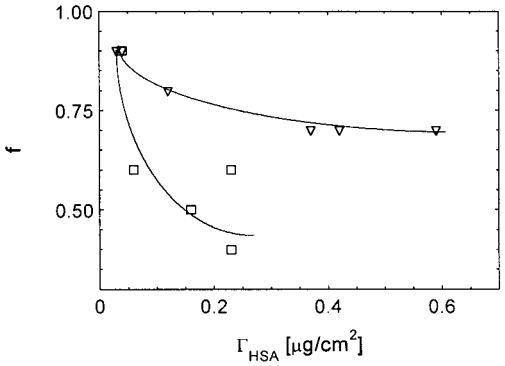

Figure 3. Mobile fraction (f) of HSA adsorbed on PAH (∇) and PSS (□) terminating films as a function of surface concentration of albumin Γ (μg/cm^2). The points represent the experimental data, the lines are drawn to guide the eye.

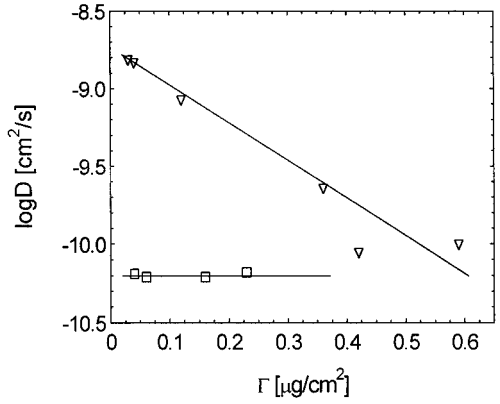

Figure 4. Logarithmic plot of the diffusion coefficients of HSA adsorbed on PAH (∇) and PSS (□) terminating films as a function of surface concentration of albumin Γ (μg/cm^2). The points represent the experimental data and the lines are drawn to guide the eye.

terminating films the diffusion coefficient of HSA strongly decreases when the protein surface concentration is increased (see Figure 4). Such an evolution is qualitatively very similar to that observed for BSA adsorbed on PMMA where the decrease of the diffusion coefficient is attributed to steric hindrance effects.[15] The diffusion coefficient of HSA on PAH ending multilayers for very small surface concentrations (intrinsic diffusion coefficient) is of the order of $(1-2) \times 10^{-9}$ cm^2/s. This value is comparable to the diffusion coefficients of BSA measured on various surfaces such as glass or PMMA.[18] Surprisingly, the diffusion coefficient of HSA on PSS terminating films is surface concentration independent over the explored surface concentration range. Moreover, its value, which is of the order of 6.4×10^{-11} cm^2/s, is much smaller than on PAH terminating films. It is also more than 1 order of magnitude smaller than the reported protein surface diffusion coefficients on solid surfaces.[18]

HSA Molecules Embedded in Polyelectrolyte Multilayers. One observes that the mobile fraction remains unchanged or decreases slightly, at least at small surface concentrations (70% compared to 90%), when HSA adsorbed on PSS ending films is embedded in −PSS−HSA−(PSS or PAH)-architectures compared to HSA adsorbed on PSS at similar surface concentrations. On the other hand the mobile fraction is considerably reduced when HSA adsorbed on PAH ending multilayers is embedded in − PAH−HSA−(PAH or PSS)-type films (30% compared to 70%). The diffusion coefficient of HSA embedded in −PAH−HSA−(PAH or PSS)-films is comparable to what is measured when HSA is adsorbed on PAH terminating films,

TABLE 2: Structural Analysis of HSA at Room Temperature under Different Conditions[a,b]

	intermolecular β-sheet		intramolecular β-sheet and/or random	α-helix	turns
HSA solution	1627	1684	1637	1653	1666
0.5 mg mL^{-1}	1.8	2.5	27.8	50.2	17.6
HSA solution	1625	1678	1637	1652	1664
1 mg mL^{-1}	5.3	3.9	29.5	41.1	20.1
−PSS−HSA	1620	1676	1637	1650	1662
0.05 mg mL^{-1}	5.9	3.7	33.6	35.0	21.7
−PSS−HSA−PSS−	1628	1680	1642	1655	1669
0.05 mg mL^{-1}	3.0	3.1	38.7	39.5	15.6
−PSS−HSA	1624	1676	1640	1654	1664
0.5 mg mL^{-1}	4.1	3.5	44.7	30.3	17.3
−PSS−HSA−PSS−	1623	1679	1637	1651	1666
0.5 mg mL^{-1}	1.7	2.4	29.8	43.4	22.7
−PAH−HSA	1622	1677	1635	1651	1664
0.05 mg mL^{-1}	4.4	3.0	30.7	42.2	19.6
−PAH−HSA−PAH−	1622	1677	1634	1649	1662
0.05 mg mL^{-1}	4.1	2.7	31.6	38.9	22.7
−PAH−HSA	1621	1677	1634	1649	1662
0.5 mg mL^{-1}	3.2	3.7	28.0	39.9	25.1
−PAH−HSA−PAH−	1622	1676	1634	1650	1663
0.5 mg mL^{-1}	3.4	4.3	30.9	43.4	17.9

[a] Gaussian-shaped component bands were obtained after Fourier smoothing of the infrared spectra as described in ref 13. [b] For simplicity, only the HSA-contacting polyelectrolytes are given for the architectures described in the Materials and Methods section. For each component band, the central frequency (cm^{-1}) and the intensity (%) relative to the total amide I intensity are given successively.

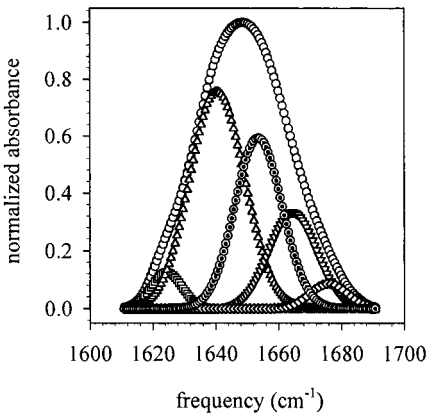

Figure 5. Relative intensities of the five component bands of the amide I region of HSA adsorbed on top of PEI−(PSS−PAH)$_2$−PSS: -o- amide I; -□- intermolecular β-sheet (1622 cm^{-1}); -Δ- intramolecular β-sheet (1637 cm^{-1}); -⊙- α-helix (1652 cm^{-1}); -∇- turns (1662 cm^{-1}); -◇- intermolecular β-sheet (1677 cm^{-1}).

considering the important variation of D in the 0.5 to 0.1 μg cm^{-2} surface concentration domain. More surprising is the increase of the diffusion coefficient when HSA adsorbed on PSS ending films (6.4×10^{-11} cm^2/s) is embedded in −PSS−HSA−(PSS or PAH)-type multilayers (1.0×10^{-10} cm^2/s).

Structure of Adsorbed or Embedded HSA Molecules "on" or "in" Polyelectrolyte Multilayers. The evolution of the mobile protein fraction on multilayer films with the protein surface concentration suggests the existence of intermolecular interactions between HSA molecules, leading to aggregation. The possible existence of such direct interactions between HSA molecules has been investigated using the amide I band of HSA as a fingerprint of its secondary structure. We used FTIR-ATR spectroscopy to this aim. The results are summarized in Table 2. Figure 5 represents a typical amide I spectrum of HSA adsorbed on a PAH terminating film. If one takes the spectrum of the 0.5 mg/mL HSA solution as a reference (spectra of

solutions of smaller protein concentrations could not be analyzed), one observes that an increase of the HSA concentration in solution or the adsorption or embedding of the proteins "on" or "in" the multilayer films is accompanied by a decrease in the α-helix content and an increase in the contribution of two bands, one at around 1620 cm^{-1} and the other near 1680 cm^{-1}. These bands are usually attributed to the existence of antiparallel intermolecular β-sheets[19] and thus suggest the presence of intermolecular interactions. For HSA adsorbed "on" or embedded "in" multilayers they represent an area of the order of 7% of the total area of the amide I band, independently of the nature of the polyelectrolyte layers in contact with the proteins. The contribution of these bands is of the order of 9% for a 1 mg/mL HSA solution and seems thus to increase with the concentration. The fact that protein embedding in the polyelectrolytes does not change significantly the amide I spectrum confirms that polyelectrolytes do not change significantly the protein's secondary structure.[12,13] The appearance of antiparallel intermolecular β-sheets in the adsorbed and embedded states must thus rather be attributed to the large local protein surface concentration than to the interactions of the HSA molecules with the polyelectrolytes. These results are qualitatively similar to those found for fibrinogen on and embedded in similar polyelectrolyte films.[13]

Discussion

One can first observe that at small HSA surface concentrations ($\approx 0.04\ \mu g/cm^2$) the diffusion coefficient is more than 1 order of magnitude smaller on PSS than on PAH ending films. Such a concentration corresponds to a surface coverage of 2.6% (respectively, 11.6%) for HSA molecules adsorbed in "end-on" (respectively, "side-on") configurations, assuming that the HSA molecules have an ellipsoidal shape of size $12 \times 2.7 \times 2.7$ nm^3.[20] When the surface concentration is increased the diffusion coefficient remains constant when HSA is adsorbed on PSS ending films and decreases significantly when the protein is adsorbed on PAH ending ones. At high surface concentrations the diffusion coefficients of HSA become of the same order of magnitude on both films. One also observes that in both cases the fraction of mobile proteins decreases from 90% to 70% (respectively, 40−50%) on PAH (respectively, PSS) ending films when the surface concentration is increased. These results may be explained as follows: When a HSA molecule comes in contact with a polyelectrolyte multilayer it interacts with the polyelectrolytes forming the outer layer of the film. These interactions take place through different charge patches distributed over the protein surface.[21] A protein such as HSA which carries a net negative charge at pH 7.4 exhibits both positive and negative patches. It can thus interact both with polyanions such as PSS or with polycations such as PAH, the overall interaction being stronger in this latter case. This is confirmed by the adsorption of HSA molecules on PSS and PAH ending films, with a higher adsorbed amounts on the polycation ending film.[22] Once adsorbed, the proteins do not stay immobile on the surface but are subject to an incessant Brownian motion so that they can become completely wrapped by the polyelectrolytes. The existence of such a wrapping of proteins by polyelectrolytes on multilayer films is confirmed by the prevention of the formation of intermolecular β-sheets between proteins on a surface even at high surface protein concentrations.[13] The interactions being strong between HSA molecules and PAH chains, it is expected that in this case the wrapping might be tight. At small coverage this should lead to a repulsive interaction similar to what is observed in steric colloidal stabilization leading only to very seldom bridging. Such a tight wrapping with few bridging has been observed in BSA/PAH solutions at low BSA mixing ratios where only small aggregates of sizes slightly larger than that of single BSA molecules could be observed.[6] When the BSA solution concentration was increased, the size of the aggregates present in the BSA/PAH solution increased, going through a maximum for a BSA/PAH mixing ratio r^* where all the BSA molecules and all the PAH chains were involved in the aggregates. The increase of the aggregate sizes as the BSA/PAH ratio increased could be fully explained by the increased importance of the bridging between the BSA molecules and the PAH chains. A similar behavior could take place on a PAH ending film when the HSA surface concentration is increased. As bridging between adsorbed HSA molecules becomes more effective, dimers, trimers, and larger aggregates appear, these entities remaining still mobile. It is expected that bridging interactions reduce the diffusion coefficient of the proteins on the surface but also that the HSA molecules involved in large aggregates appear immobile at our experimental time scale. This could explain the presence of two populations of adsorbed HSA molecules, the immobile one corresponding to the molecules involved in the largest aggregates. The fact that the diffusion coefficient decreases when the HSA coverage increases on PAH ending films is thus due to a more effective bridging as the HSA/PAH ratio increases on the surface. The wrapping of the HSA molecules by PSS chains should be much looser than by PAH ones due to weaker interactions. It is thus expected that bridging between HSA molecules sets in, in this case, already at low HSA coverage. The counterpart of this effect in solution should be the observation of large PSS/HSA aggregates at HSA/polyelectrolyte mixing ratios quite smaller with PSS than with PAH. Unfortunately, to our knowledge such experiments were not reported, up to now, in the literature. Here too, as the protein surface concentration is increased, larger aggregate buildups lead to a protein population that appears immobile. In such aggregates direct protein interactions leading to the formation of intermolecular β-sheets should be favored, as it is observed by ATR. The smaller mobile fraction at a given coverage, observed on PSS ending films when compared to PAH ending ones could thus be due to the fact that on PAH ending films the tight wrapping partially prevents intermolecular bridging. It must be pointed out that other explanations of the observed features may be possible but further experiments must be performed to enter deeper in the interpretation.

One also observes that when HSA is embedded in multilayers the diffusion behavior depends mainly on the nature of the polyelectrolyte on which it is first adsorbed. When HSA is embedded in −PAH−HSA-(PAH or PSS)- films the mobile fraction decreases significantly. The diffusion coefficient of the 30% mobile fraction remains close to what is observed for HSA adsorbed on PAH terminating films. This may be due to the fact that the HSA molecules are strongly wrapped by the PAH chains. These chains are thus highly constrained and do not easily entangle with polyelectrolyte chains that are deposited subsequently on the film. When HSA is embedded in −PSS−HSA−(PSS or PAH)-films the mobile fraction remains unaffected by the further polyelectrolyte adsorption and the diffusion coefficient is protein concentration independent. Surprisingly it becomes even faster than for HSA adsorbed on PSS terminating films. This may be due to the fact that when polyelectrolytes are deposited on the −PSS−HSA-film, HSA interacts mainly with the PAH that is deposited on the top (even if a PSS layer was first deposited). PAH may partially exchange

PSS chains interacting with the HSA molecules and reduce the interaction of the HSA molecules with the underlying PAH chains. As a consequence their diffusion coefficient should increase as observed.

Acknowledgment. This work was supported by the program "Adhésion Cellules-Matériaux" and by the program CNRS "Physique et Chimie du Vivant". It was performed within the framework of the CNRS/INSERM Research Network "Mécanismes physico-chimiques d'adhésion cellulaire: forces d'adhésion entre ligands et récepteurs biologiques". We are grateful to Prof. G. Decher for stimulating discussions about polyelectrolyte multilayers.

References and Notes

(1) Chluba, J.; Voegel, J.-C.; Decher, G.; Erbacher, P.; Schaaf, P.; Ogier, J. *Biomacromolecules* **2001**, *2*, 800.

(2) Caruso, F.; Niikura, K.; Furlong, D. N.; Okahata, Y. *Langmuir* **1997**, *13*, 3427.

(3) Brinda, E.; Houska, M. In *Protein Architecture, Interfacing Molecular Assemblies and Immobilization Biotechnology*; Lvov, Y., Möhwald, H., Ed.; Marcel Dekker: New York, 2000; p 251.

(4) Ariga, K.; Kunitake, T. In *Protein Architecture, Interfacing Molecular Assemblies and Immobilization Biotechnology*; Lvov, Y., Möhwald, H., Eds.; Marcel Dekker: New York, 2000; p 169.

(5) Mascotti, D. P.; Lohman, T. M. *Proc. Natl. Acad. Sci. U.S.A.* **1990**, *87*, 3142.

(6) Ball, V.; Winterhalter, M.; Schwinte, P.; Lavalle, Ph.; Voegel, J.-C.; Schaaf, P. *J. Phys. Chem. B* **2002**, *106*, 2357.

(7) Kaibara, K.; Okazaki, T.; Bohidar, H. B.; Dubin, P. L. *Biomacromolecules* **2000**, *1*, 100.

(8) Ladam, G.; Schaaf, P.; Cuisinier, F. J. G.; Decher, G.; Voegel, J. C. *Langmuir* **2001**, *17*, 878.

(9) Ladam, G.; Schaad, P.; Voegel, J. C.; Schaaf, P.; Decher, G.; Cuisinier, F. *Langmuir* **2000**, *16*, 1249.

(10) Appleton, B.; Gibson, T. D.; Woodward, J. R. *Sensors Actuators B* **1997**, *43*, 65.

(11) Gibson, T. D.; Hulbert, J. N.; Pierce, B.; Webster, J. I. In *Stability and Stabilisation of Enzymes*; van den Tweel, W. J. J., Harder, A., Buitelaar, R. M., Eds.; Elsevier: Amsterdam, 1993; p 337.

(12) Müller, M.; Rieser, T.; Dubin, P. L.; Lunkwitz, K. *Macromol. Rapid Commun.* **2001**, *22*, 390.

(13) Schwinté, P.; Voegel, J. C.; Picart, C.; Haikel, Y.; Schaaf, P.; Szalontai, B. *J. Phys. Chem. B* **2001**, *105*, 11906.

(14) Szyk, L.; Schaaf, P.; Gergely, C.; Voegel, J. C.; Tinland, B. *Langmuir* **2001**, *17*, 6248.

(15) Tilton, R. D.; Gast, A. P.; Robertson, C. R. *Biophys. J.* **1990**, *58*, 1321.

(16) Davoust, J.; Devaux, P. F.; Leger, L. *EMBO J.* **1982**, *1*, 1233.

(17) Goormaghtigh, F.; Cabiaux, V.; Ruysschaert, J.-M. In *Subcellular Biochemistry, Vol. 23: Physicochemical Methods in the Study of Biomembranes*; Hilderson, H. J., Ralston, G. B., Eds.; Plenum Press: New York, 1994; p 405.

(18) Tilton, R. D. In *Biopolymers at Interfaces*; Malmstem, M., Ed.; Surfactant Science Series; Marcel Dekker: New York, 1998; Vol. 75, p 363.

(19) Green, R. J.; Hopkinson, I.; Jones, R. A. L. *Langmuir* **1999**, *15*, 5102.

(20) Haynes, C. A.; Sliwinski, E.; Norde, W. *J. Colloid Interface Sci.* **1994**, *164*, 394.

(21) Mattison, K. W.; Dubin, P. L.; Brittain, I. J. *J. Phys. Chem. B* **1998**, *102*, 3830.

(22) Ladam, G.; Gergely, C.; Senger, B.; Decher, G.; Voegel, J.-C.; Schaaf, P.; Cuisinier, F. J. G. *Biomacromolecules* **2000**, *1*, 674.